Available online at www.sciencedirect.com
SCIENCE DIRECT®
Control Engineering Practice 13 (2005) 291–303
CONTROL ENGINEERING PRACTICE
www.elsevier.com/locate/conengprac

Impedance control for a pneumatic robot-based around pole-placement, joint space controllers

Robert Richardson[a,*], Michael Brown[b], Bipin Bhakta[c], Martin Levesley[d]

[a] Department of Computer Science, University of Manchester, M13 9PL Manchester, UK
[b] WS Atkins Consultants Ltd., 220 Aztec West, Park Avenue, Almondsbury, Bristol, UK
[c] Rheumatology and rehabilitation research unit, University of Leeds, UK
[d] School of Mechanical Engineering, University of Leeds, UK

Received 19 December 2002; accepted 19 March 2004

Available online 10 May 2004

Abstract

Traditionally the control of pneumatic actuators has been limited to movement between pre-set stops or switches. Modern pneumatic systems exhibit great power to weight ratio, are backdrivable and can be precision controlled. As such these actuators offer great advantages over direct drive electric motors for robotic devices.

Increasingly robots are required to interact directly with humans requiring control of not only the robot position but also taking into account the applied forces. Robotic physiotherapy is one such application. This paper describes the implementation of a force and position control strategy, termed impedance control, on a pneumatic robot designed to implement robotic physiotherapy. The controller is shown to work appropriately over a range of conditions. The performance achieved is limited by the quality of force measurement in multiple axes.

Keywords: Pneumatic systems; PID controllers; Position control; Force control; Impedance control; Model-based control

1. Introduction

Many people suffer from debilitating illnesses such as stroke. These patients require physiotherapy to aid towards full or partial recovery of any effected limbs, however patients often do not receive an optimum amount of exercise due to resource limitations. Robots would be able to administer physiotherapy for greater periods of time more consistently. In this situation robots are connected directly to humans. This level of intimacy requires safe interaction where the robot does not dominate the partnership. In this robotic physiotherapy context the robot guides the patient's limb through a pre-set series of motions, applying forces to gently assist the patient's limb movement, rather than dominate it.

Several force and position control schemes have been devised for robotic interaction tasks. Chiavervini and Sciavicco (1993) proposed a parallel approach to force and position control, where position trajectories are sacrificed due to force demands. For physiotherapy, specifying specific position demands would be difficult, as they would be masked by the dominance of the force loop. Ferretti, Magnani, and Rocco (1997) proposed a hybrid force/position control strategy for robots with multiple degrees of freedom. Force is controlled in constrained directions, while position is controlled in unconstrained directions. With the robot operating in a constrained environment the controller would behave purely as a force controller. Schutter and Brussel (1987) used a position control strategy combined with an external force loop to alter demand position and velocity. An extension to this was devised by Hogan (1985) who developed a force/position control strategy, termed 'impedance control', for which the desired force and position are connected through mass, spring and damper characteristics. Several prototype physiotherapy robots use this technique for robot and human interaction. Krebs, Hogan, Aisen, and Volpe (1998) have

*Corresponding author. Tel.: +44-161-275-6169.
E-mail address: rob@cs.man.ac.uk (R. Richardson).

0967-0661/$ - see front matter © 2004 Elsevier Ltd. All rights reserved.
doi:10.1016/j.conengprac.2004.03.011

implemented force-based impedance control on a low inertia prototype physiotherapy robot-based upon electric motors. Noritsugu and Yamanaka (1996) have used position-based impedance control on a rubber artificial muscle (RAM) for a prototype physiotherapy robot, incorporating addition pressure controllers to ensure pressures within the RAM are accurately controlled.

Recent developments in pneumatic actuators and valves allow them to be considered for applications which previously only electric motors were suitable. Using pneumatic actuators to implement impedance control has major benefits. Pneumatic system's inherent low stiffness and direct drive capabilities enable smooth compliant motion, which is difficult to obtain from conventional geared electric motor systems. Moreover, pneumatic actuators can cost up to 10 times less than electric motors, while offering a higher power to weight ratio.

Most impedance controllers are designed around force loops, which make use of the ability of an electric motor to supply torque on demand (Krebs et al., 1998). Pneumatic and hydraulic actuators could also be used. However, due to factors such as fluid compressibility, stiction and viscous friction, accurate positioning of hydraulic and pneumatic systems is difficult to obtain from a force-based control system. Moreover, an accurate model of the system dynamics is required, which can be difficult to obtain (Heinrichs, Sepehri, & Thorton-Trump, 1997). Indeed, Krebs et al. (1998) used a low inertia manipulator to reduce the influence of system dynamics. Generally, the inertial dynamics of the manipulator are significant. A position based impedance controller does not require consideration of the system dynamics. Heinrichs et al. (1997) proposed a position based impedance controller for an existing hydraulic industrial robot, validating their work experimentally. Gorce and Guihard (1999) propose a multi-link, position based impedance controller for implementation on a legged robot. They use an actuator model to predict the torque produced from the pneumatic cylinders. The performance of the controller is demonstrated through simulation.

In this paper an impedance control strategy is implemented on a pneumatic robot to implement physiotherapy. The impedance controller is validated through multiple tests of a human applying forces to the robot end-point, while varying the impedance characteristics, as would occur in robotic physiotherapy. Section 2 describes the pneumatic robot and its workspace. Section 3 implements PID joint space control demonstrating a linearising compensation scheme to negate the effect of the cylinder angle of action. Data from the PID control is used to implement pole-placement joint space position control in Section 4. A demand filter in the pole-placement controller is used to reduce the controller response to noise. Section 5 examines the pole-placement response of the two degree-of-freedom (d.o.f.) robot to global position demands. Section 6 implements the impedance controller on the two d.o.f. robot and finally Section 7 draws conclusions from the work.

2. The physiotherapy robot

A three d.o.f. robot has been developed to administer robotic physiotherapy (Fig. 1). A custom made three d.o.f. force sensor measures the contact force between the robot and human. The workspace of the robot is shown in Fig. 2 along with typical hand movement envelope. Each joint is revolute and actuated by a pneumatic actuator system consisting of a low friction pneumatic cylinder and two electro-pneumatic valves. The low friction cylinder minimises stiction effects enabling accurate control (Richardson, Plummer, & Brown, 2001) and each valve supplies regulated pressure to a single chamber of the pneumatic cylinder. This enables the pressure difference across the cylinder to be specified by software changes alone and also allows the individual chamber pressures to be regulated by the

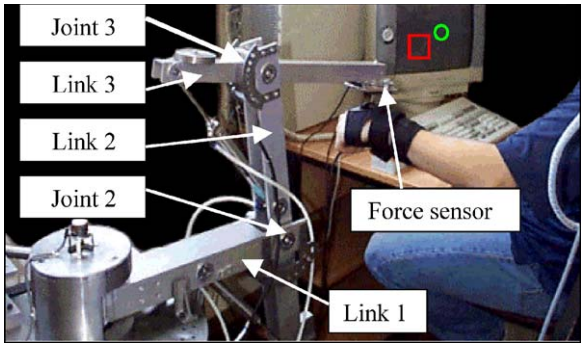

Fig. 1. Physiotherapy robot.

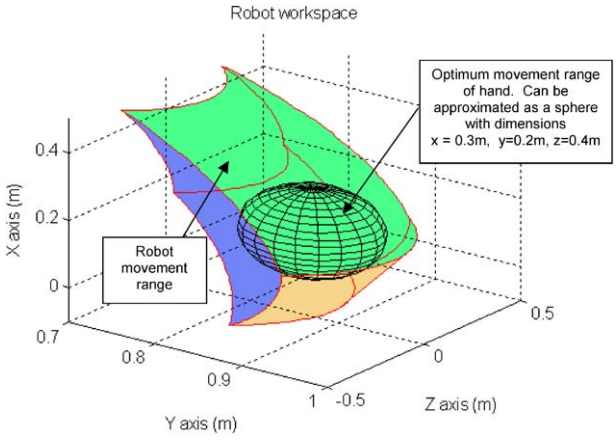

Fig. 2. Robot workspace.

valves themselves, avoiding the need for additional pressure control that has been implemented, for example, in Liu and Bobrow (1988). To achieve accurate control, it is desirable to control both valves from a single control signal. This has been achieved through the use of an equilibrium pressure for which one valve has pressure increased and the other valve has pressure decreased (Richardson et al., 2001). Thus, through manipulation of a single control voltage, the output force and, hence link position can be altered.

The robot is constructed with counterbalance weights on each joint to reduce the effect of gravity on the robot movement. The robot configuration makes it impossible to completely compensate for gravity effects, therefore the position controllers are required to operate with some gravity forces present. It is possible to compensate for gravity effects using only actuator forces at each joint. However, this would result in large control signals applied to the actuators under stationary conditions and the possibility of actuator saturation during motion.

3. PID joint space control

To achieve global position objectives each joint is controlled to achieve a specified angle based upon the inverse kinematics of the robot. Fig. 3 demonstrates the physical system to be controlled for one link of the robot.

The pneumatic cylinder extends linearly with its applied force-causing link 3 to rotate. As a result of the robot physical configuration the force exerted on link 3 to rotate it depends not only upon the actuator force output but also upon the joint angle. This phenomenon results in different angular acceleration of the link depending upon the link position, for identical force output from the pneumatic cylinder. The non-linearity manifests itself as an apparent increase in gain for negative angles. A single PID controller controls the individual joint angles. The PID gains for each joint were optimised using the downhill simplex method (Richardson, Brown, Bhakta, & Levesley, 2003). The integral squared time-weighed error (ISTE) of the demand position and actual position, produced a cost for each response that the controller optimised. The optimised PID controller achieved adequate performance (Fig. 4). However, the non-linearity caused by changes in angle C_3 (Fig. 3) degrades the controller performance and renders the system unsuitable to implement linear model-based control such as pole-placement. As the angle C_3 can be calculated it is possible to include a trigonometric linearising function that can be considered to be part of the plant, causing the input voltage and output torque to behave in a more linear manner (Fig. 5). Where U_{des} is the control output from the PID controller, U_{act} is the control input to the pneumatic system, θ_{3d} is the desired angle and θ_3 is the actual joint angle. Including the linearising element amplifies the system gain, requiring the PID gains to be optimised again. The resultant link step response is shown in Fig. 4 for optimised PID with and without linearising element.

The linearised controller demonstrates improved linearity with the overshoot and oscillation almost identical for the positive and negative steps. It is

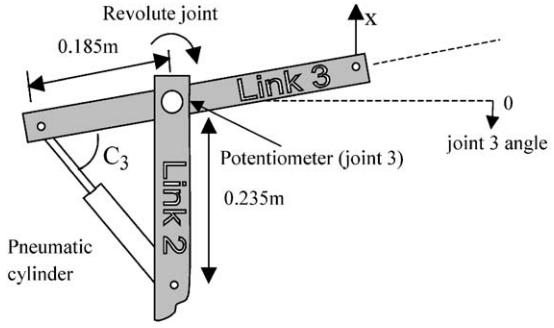

Fig. 3. Links 2 and 3 of the physiotherapy robot.

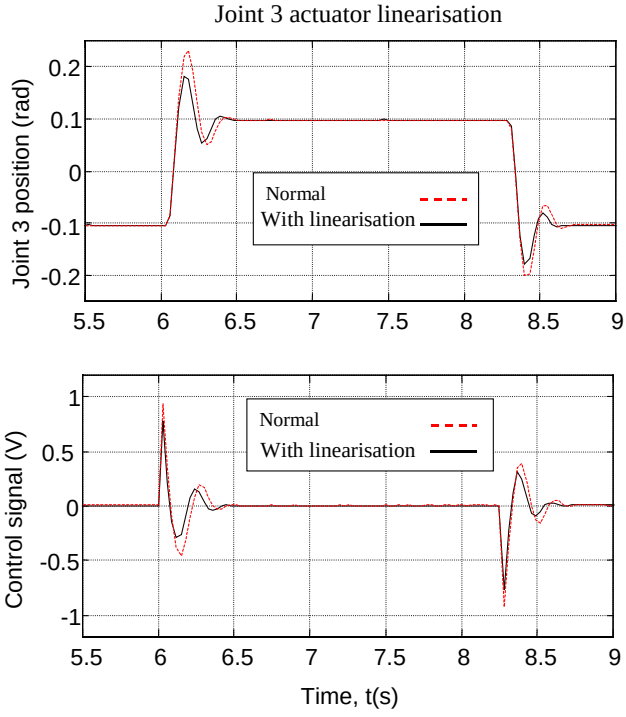

Fig. 4. Optimised joint 3 response with and without linearising element.

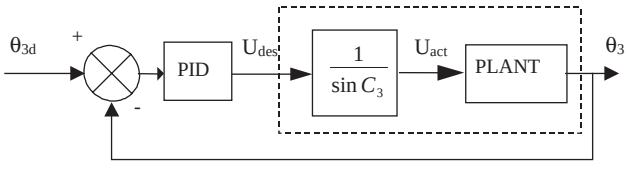

Fig. 5. Improving system linearity.

interesting to note that the overall performance of the controller has improved due to the increased linearity enabling the optimisation strategy to tune the gains with greater accuracy.

4. Pole-placement joint space control

Using the input/output data of the optimised PID with linear element, a plant model was calculated using least-squares parameter estimation:

$$\theta_3 = \frac{B(z)}{A(z)} u_{des} = \frac{0.0845 z^{-2}}{1 - 1.76 z^{-1} + 0.76 z^{-2}} u_{des}, \quad (1)$$

where θ_3 is the joint angle (rad) and u_{des} is the control signal (V). Note it has been demonstrated that this model order is appropriate for this pneumatic valve and cylinder (Richardson et al., 2001) due the valves approximating to a zero-order response. Using this plant model the coefficients $F(z^{-1})$ and $G(z^{-1})$ were calculated for specific closed loop poles by solving the diophantine equation (Astrom & Wittenmark, 1997).

Due to the susceptibility of the potentiometers to noise, the closed loop poles for conventional pole-placement control are required to be slow to provide adequate robustness, severely limiting the performance of the controller. However, it is possible to augment a standard pole-placement controller with a demand filter (H) to attenuate the controller's response to noise (Fig. 6). Where θ_{3d} is the demand input, e_t is the measurement noise and θ_3 is the actual position.

Obtaining a transfer function of the controller in Fig. 6, demonstrates the H filter only appears in the part of the transfer function that connects errors in measurement and output response (Vaughan & Plummer, 1990)

$$y_t = \frac{B(z^{-1})}{A_m(z^{-1})} r_t + \frac{F(z^{-1})A(z^{-1})}{A_m(z^{-1})H(z^{-1})} e_t. \quad (2)$$

Selection of closed-loop poles for pole-placement is always a trade off between speed of response and robustness to measurement noise. Section of closed loop poles at $0.3 \pm 0.05i$, to obtain a fast response, result in the standard pole-placement controller (without H filter) being very sensitive to measurement noise. Specifying the H filter as a first-order low pass filter with a cut off frequency at 6 Hz significantly reduces the controller response to measurement noise. Experimental results of the robot joint 3 response (the angle between link 2 and link 3) with and without the demand filter show the response time and overshoot to be consistent, however the steady-state response to noise is almost completely removed when the H filter present (Fig. 7). This lack of response to measurement noise is best illustrated by examining the control signal high frequency oscillation for the standard pole-placement controller (Fig. 7). A similar linearisation process can be performed on the second joint (the angle between link 2 and link 1) of the pneumatic robot (Richardson, 2001).

5. Two d.o.f. pole-placement position response

The two joint space controllers, acting on joints 2 and 3 can be combined using inverse kinematics to control the global position of the robot end-point in two d.o.f. (x, y). To test the performance of the robot it was programmed with a trajectory that causes it to extend horizontally in the y direction and then retract to its original position, while only moving slightly in the x direction (Fig. 8).

The global desired and experimental x and y position and velocities are shown in Fig. 9. The velocity is obtained by differentiation of the angular position reading from the potentiometers, and as such is susceptible to measurement noise. The position tracking of the robot is not exact with the worst tracking resulting in approximately 5 mm error. This level of error is acceptable in the final device as the accuracy of human motion is low. The quality of response could be improved by increasing the speed of the system poles in the pole-placement joint space controllers, however this would result in controller output saturation, potentially causing controller instability. A saturation compensated pole-placement controller could allow the pole-placement controller to operate within this saturation region (Ling & Plummer, 1999).

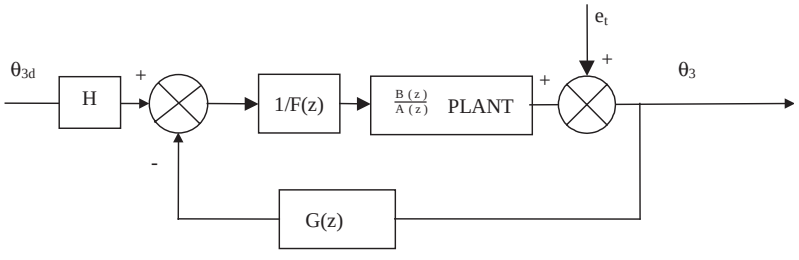

Fig. 6. Pole-placement control.

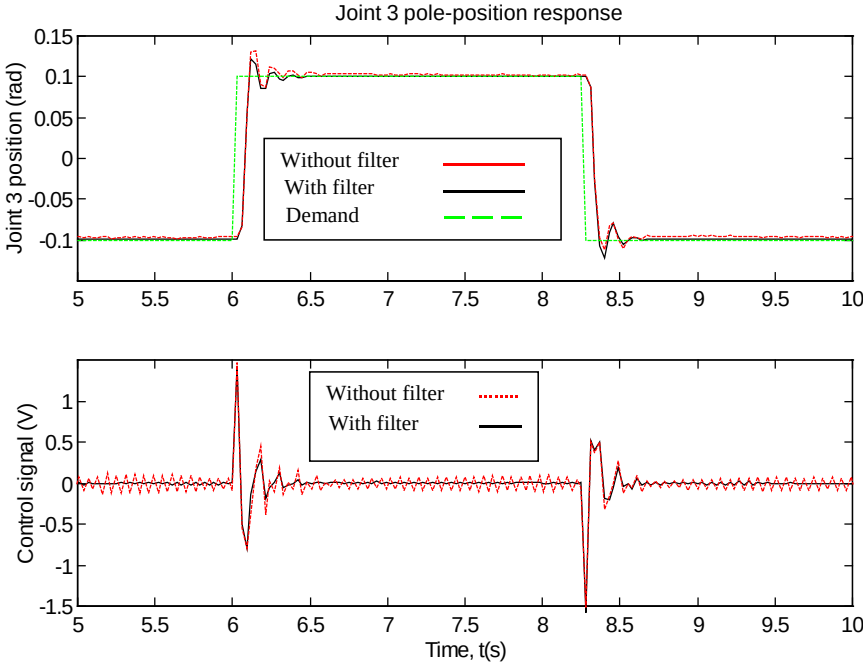

Fig. 7. Pole-placement joint space response with and without demand filter.

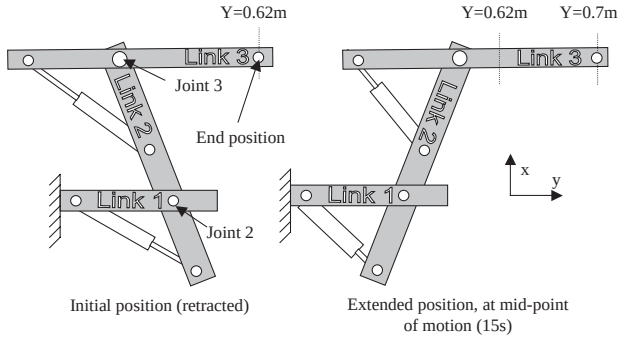

Fig. 8. Robot configuration in retracted and extended.

6. Impedance control

Position control is not appropriate for physiotherapy, where the relationship between external forces and position (the 'feel' of the robot to the patient) is required to be directly specified. Impedance control has been developed over the last decade to enable robots to smoothly move between contact and non-contact phases of motion. Examining how humans interact with their environment was an integral part of this development. Impedance control fixes the relationship between the manipulator end-point and external forces as mass, spring and damper system. This transfer function for position-based impedance control (sometimes termed admittance control) can be specified in the s-domain as:

$$\frac{x_i}{F_x} = \frac{1}{Ms^2 + Cs + K}, \tag{3}$$

where x_i is the change in position due to external force (F_x), M is the inertial component, C is the damping component and K is the stiffness component.

Rearranging Eq. (3) so that position becomes the input (known as force-based impedance control) gives:

$$\frac{F_x}{x_i} = Ms^2 + Cs + K. \tag{4}$$

Eqs. (3) and (4) are known as the duality of impedance control. These two subtly different approaches require different controller structures. A more detailed discussion of these differences can be found in Richardson (2001), but a summary of the advantages and disadvantages of each type of impedance controller is given in Table 1. As highlighted by Heinrichs et al. (1997), position-based impedance control (admittance control) is more appropriate for pneumatic systems. To implement position-based impedance control, Eq. (3) is implemented. A multiple d.o.f. force sensor measures contact forces which are then fed into the impedance filter. The output of the filter is the required change in global position due to the external force.

As mentioned in Table 1 to implement position-based impedance control requires a position controller that is robust to external force disturbances. The backdrivable nature of pneumatic cylinders results in the position controllers having little robustness to externally applied forces. Indeed, significant position control errors occur for varying externally applied force. Often, these externally applied forces are unknown, and as such cannot be directly compensated for. In this situation the force sensor measures the externally applied forces,

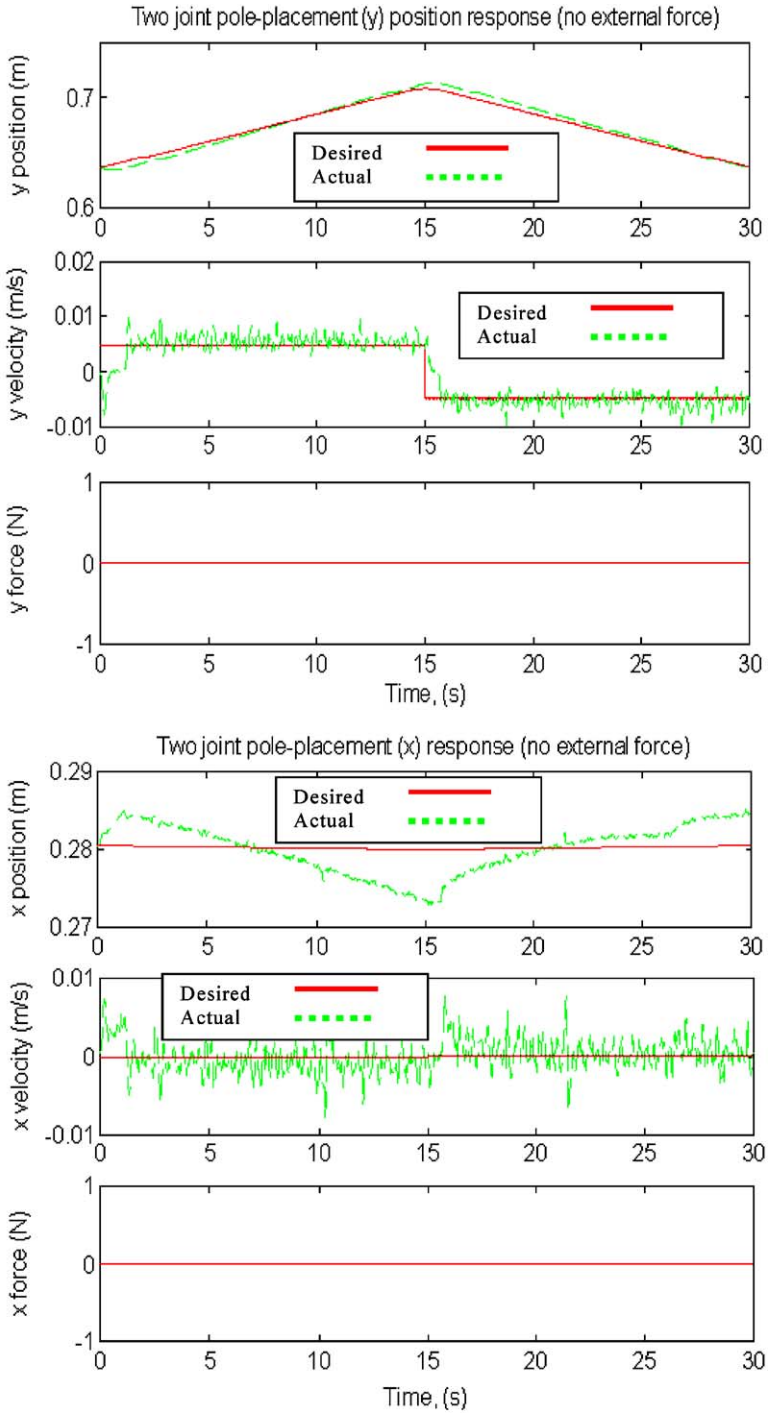

Fig. 9. Two d.o.f. pole-placement position response.

allowing the addition of a feed-forward force element to improve the performance (Richardson, Brown, & Plummer, 2000). Measured forces are converted into voltage control signals, which are directed straight to the pneumatic system. The valves are pressure proportional so this open-loop voltage produces a force to balance the externally applied force.

The effect of the feed-forward force element is to reduce the backdrivable properties of the robot. However, it should be remembered that although the direct effect of the external force is negated, the measured force results in the position control-loop implementing a new position, specified by the impedance filter characteristics. Therefore the desired impedance characteristics are achieved.

A flow chart of the multiple d.o.f. controller is shown in Fig. 10. The desired end point trajectory is specified before implementing the controller, in the form of global

Table 1
Comparison of admittance control and impedance control

	Admittance control	Impedance control
Advantages	Most appropriate for environments consisting of stiffness and damping elements. Only requires addition of a force sensor on conventional robotic devices based around measurement of link position.	Most appropriate for environments consisting of inertial element. Easy to implement on direct-drive electric motor systems due to the ease at which torque can be controlled during motion.
Disadvantages	Requires a high gain position controller robust to external force disturbances	Difficult to implement on actuator systems where force output is effected by robot movement. Requires robot inertial model, which can be difficult to obtain.

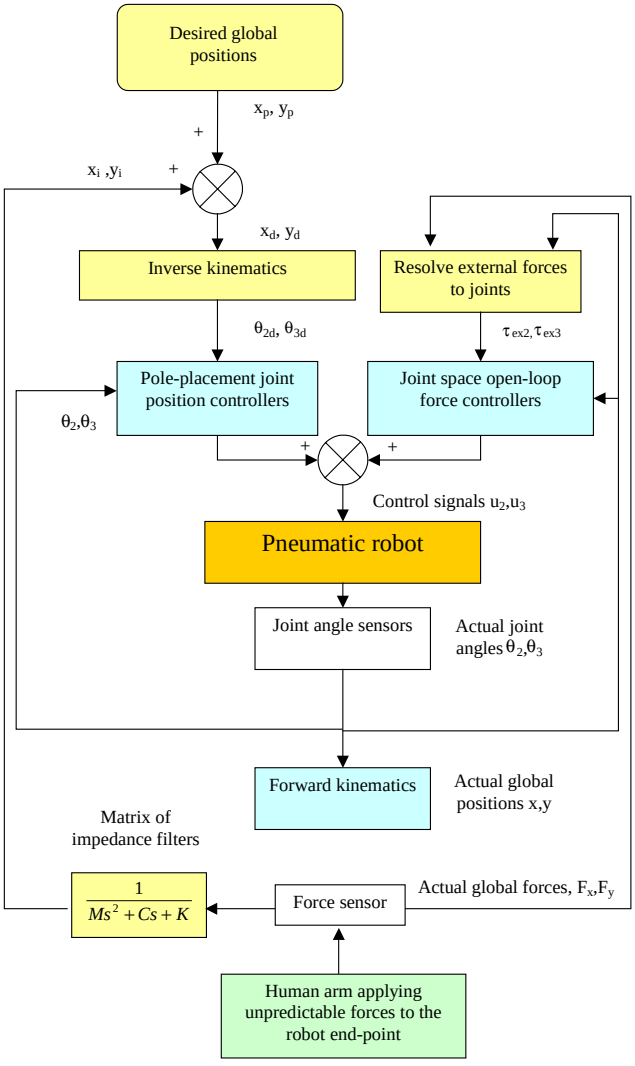

Fig. 10. Implementing impedance control in multiple d.o.f.

position co-ordinates (x_p, y_p). These co-ordinates, when added to the desired change in position due to external forces (as a result of the impedance filter) (x_i, y_i), form the desired robot position at any instant. The desired global positions are converted into joint space demands (θ_{2d}, θ_{3d}), using the robot inverse kinematics. Two independent controllers implement the desired joint space positions.

External forces are resolved through the robot to obtain their influence on each joint (τ_{ex2}, τ_{ex3}). An equal, but opposite force is generated by the joint space open-loop force controllers, to reduce the effects of these external forces on link position.

The forward kinematics of the joint positions reveal the robot end position in task space co-ordinates (x, y). External forces are measured at the robot end-point using a multiple axis force sensor (Richardson et al., 2003). Separate impedance filters convert the global external forces F_x and F_y into changes of the x and y desired task space co-ordinates, respectively. Note that it is possible to implement different impedance filters for different d.o.f. enabling one d.o.f. to be stiff while another is compliant. The mass element is used in haptic interfaces where the robot is required to mimic the physical characteristics of objects.

In the physiotherapy context only stiffness and damping is required to move the arm to the correct trajectory. When subjects experience difficulty following a predefined trajectory, a force will exist between the human limb and robot. Due to the impedance control strategy this force is dependent on the stiffness and damping parameters specified. To assess the controller performance, five alternative stiffness and damping parameters were assessed. Due to the inertia of the robot links and delays in the robot response it is not possible to implement zero damping and stiffness (this would result in zero force for any movement of the robot end-point). A stiffness value of 50 N/m and damping of 50 N/ms represents the approximate minimum values (test 1). Test 2 increases the stiffness to 170 N/m while maintaining damping at 50 N/ms. This assesses the performance of increased stiffness that would be used in a physiotherapy context, to increase the force towards the desired trajectory if the patient was experiencing difficulty. Test 3 implements a stiffness of 50 N/m with damping of 170 N/ms. The increased damping here could be used to reduce tremor that may be present in a patients motion. Test 4 increases the stiffness to 250 N/m and damping to 250 N/ms. This is

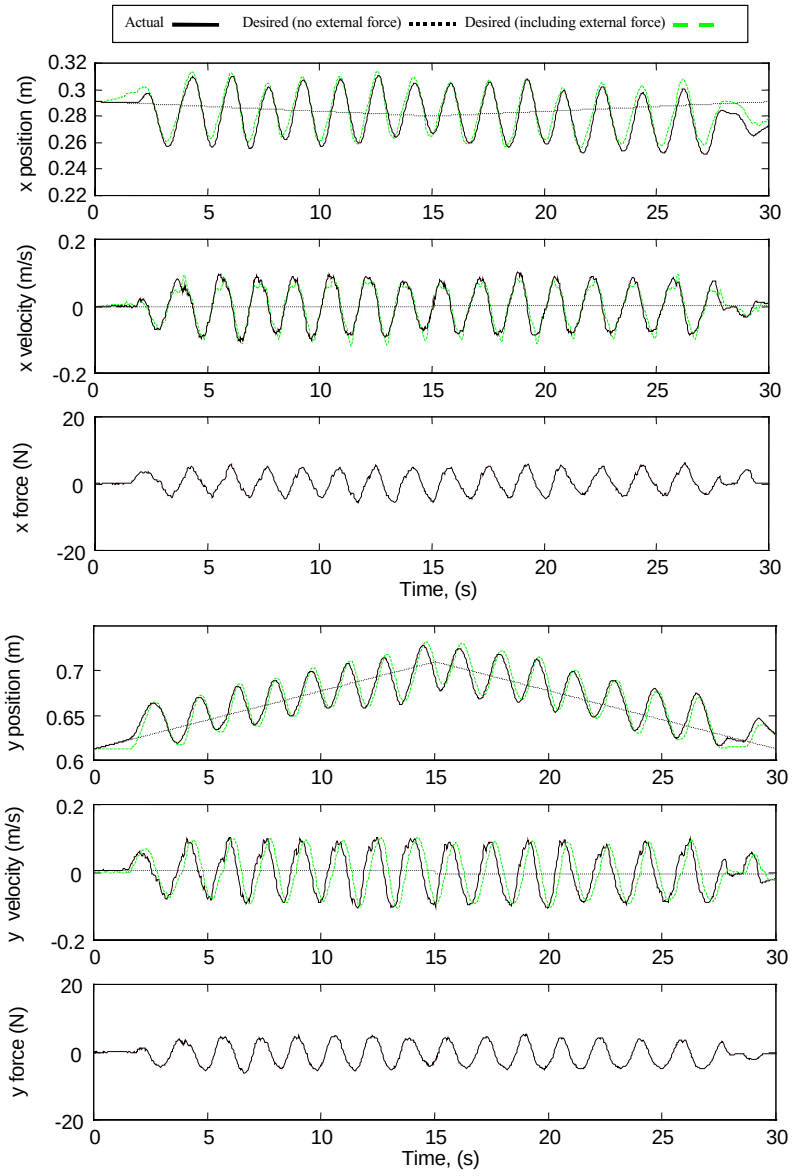

Fig. 11. Pole-placement impedance controller ($K = 50$, $C = 50$).

designed to be an extreme test of controller performance with large forces resulting in little displacement. These are likely to be the largest values use due to the strength and weight of the human arm combined with the motion of the robot. Finally test 5 implements a stiffness of 130 N/m and a damping of 130 N/ms to test the controller performance at around the middle of the available stiffness and damping parameters. For all of these experiments a circular force crossing the $x-$ and y-axis was applied by a human subject, resulting in sinusoidal forces in the x and y direction.

Note there are now three graphs to demonstrate the performance. The desired trajectory of the robot end-point if no force is applied to the robot.

The robot desired position altered due to the external force depending upon the specified damping and stiffness parameters and finally the actual robot position. Note if the robot tracking was perfect the robot end position would be identical to the desired position incorporating the external force. Below is a summary of the performance of each test.

Test 1. *K=50, C=50 (Fig. 11)*: Sinusoidal forces of ± 8 N are applied in x and y to the robot end-point while it extends and retracts in the y-plane. A small delay is present in the x position response, however the magnitude of the response is correct. The velocity of the x plane is also accurately tracked. A similar performance is found in the y response with the robot extending and retracting while accurately behaving with the correct stiffness and damping due to the external forces.

Test 2. K=170, C=50 (Fig. 12): Sinusoidal forces of ± 8 N are applied in x and y to the robot end-point while

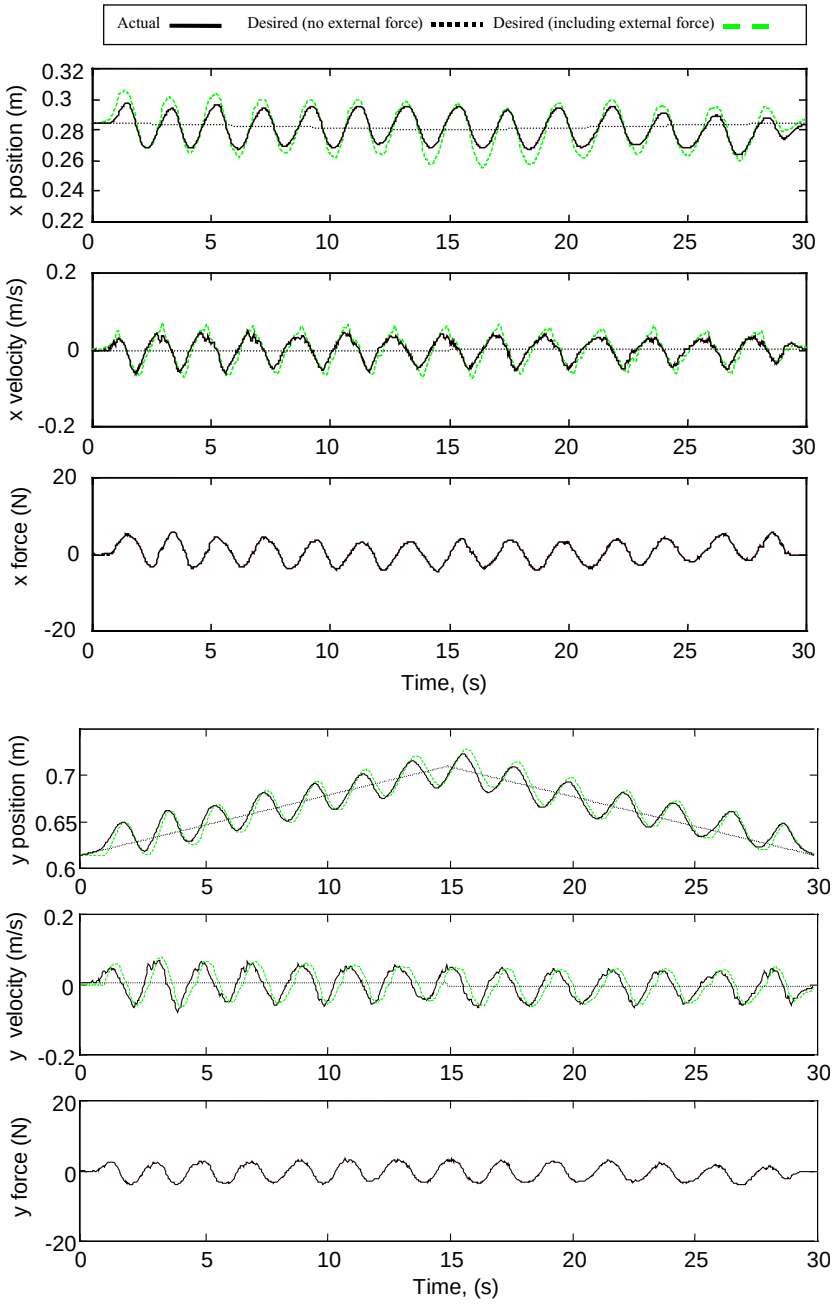

Fig. 12. Pole-placement impedance controller ($K = 170$, $C = 50$).

it extends and retracts in the y-plane. The x position tracking has the correct shape however the magnitude of the motion is less than the desired. This is likely to be due to errors in force measurement as the multiple axis force sensor has been shown to be susceptible to input torque. The y response is again accurate with the position response slightly delayed.

Test 3. K=50, C=170 (Fig. 13): Sinusoidal forces of ± 8 N are applied in x and y to the robot end-point while it extends and retracts in the y-plane. Due to the increased damping the number of force cycles the subject has applied to the robot end-position has decreased. The increased damping results in less delay between the desired and actual position response. Again the x position response has the correct shape but errors in the magnitude due to input torque effecting force measurement.

Test 4. K=250, C=250 (Fig. 14): Increasing the stiffness and damping results in the subject experiencing difficulty applying external forces to the robot end-point which are large enough to assess the controller performance. Due to this approximate sinusoidal forces of ± 15 N were applied in the x and y plane. This represents the most extreme test of controller

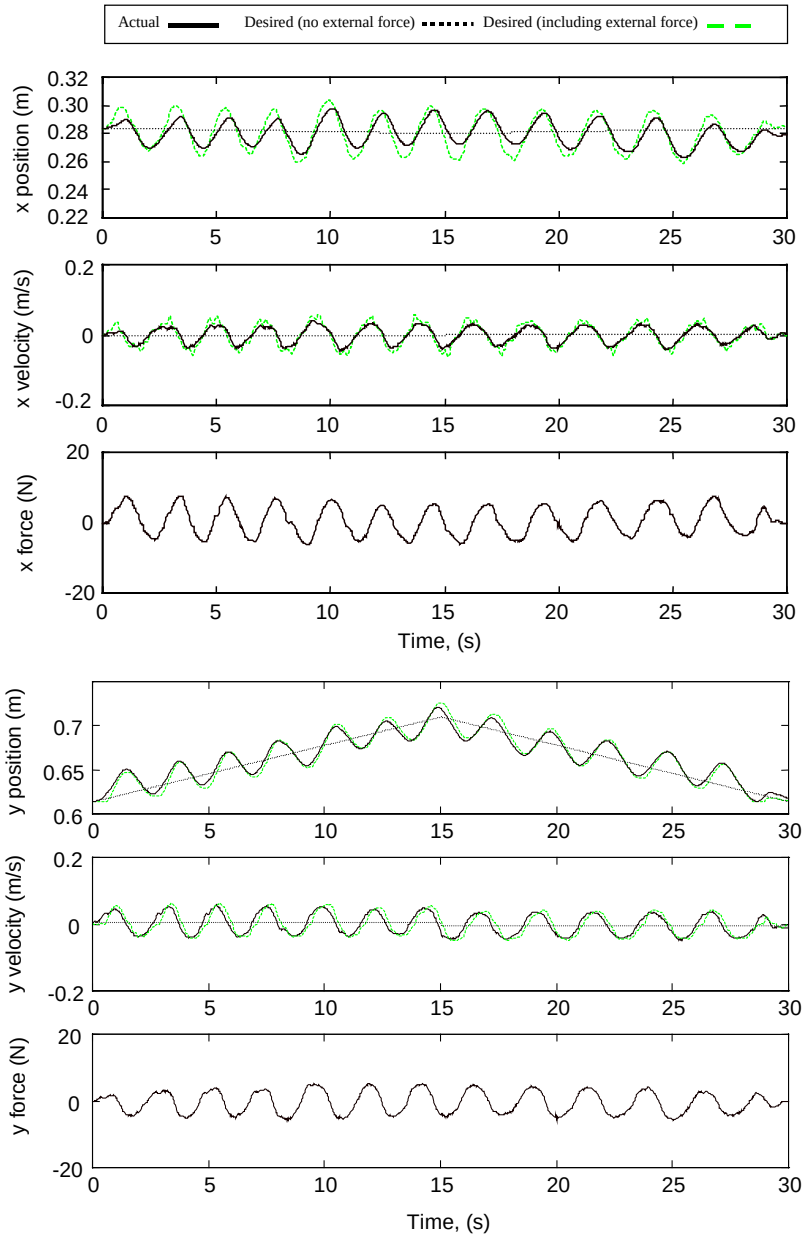

Fig. 13. Pole-placement impedance controller ($K = 50$, $C = 170$).

performance with the controller required to accurately control the position while balancing these external forces. Both the x and y responses are accurately tracked with the magnitude of the x position response now greater than required.

Task 5. K=130, C=130 (Fig. 15): Sinusoidal forces of ± 12 N are applied in x and y to the robot end-point. The reduction in the stiffness and damping parameters from task 4 enables an improvement in the sinusoidal input force. The position tracking is worse than that of task 1 due to the increased input forces. However both the x and y responses have approximately the correct magnitude and shape.

The results show the robot capable of implementing an impedance control strategy with varying stiffness and damping parameters. These experiments have highlighted the requirement for accurate force measurement which is not susceptible to input torque's. Moreover any noise from the force sensor is fed directly to the pneumatic cylinder due to the force balancing strategy and also into the demand position. This can result in vibration at the robot end-point. This is particularly apparent when large input forces are applied. These results also highlight the need to assess any impedance control strategy across a range of impedance's as it is highly likely that performance will be impedance parameter specific.

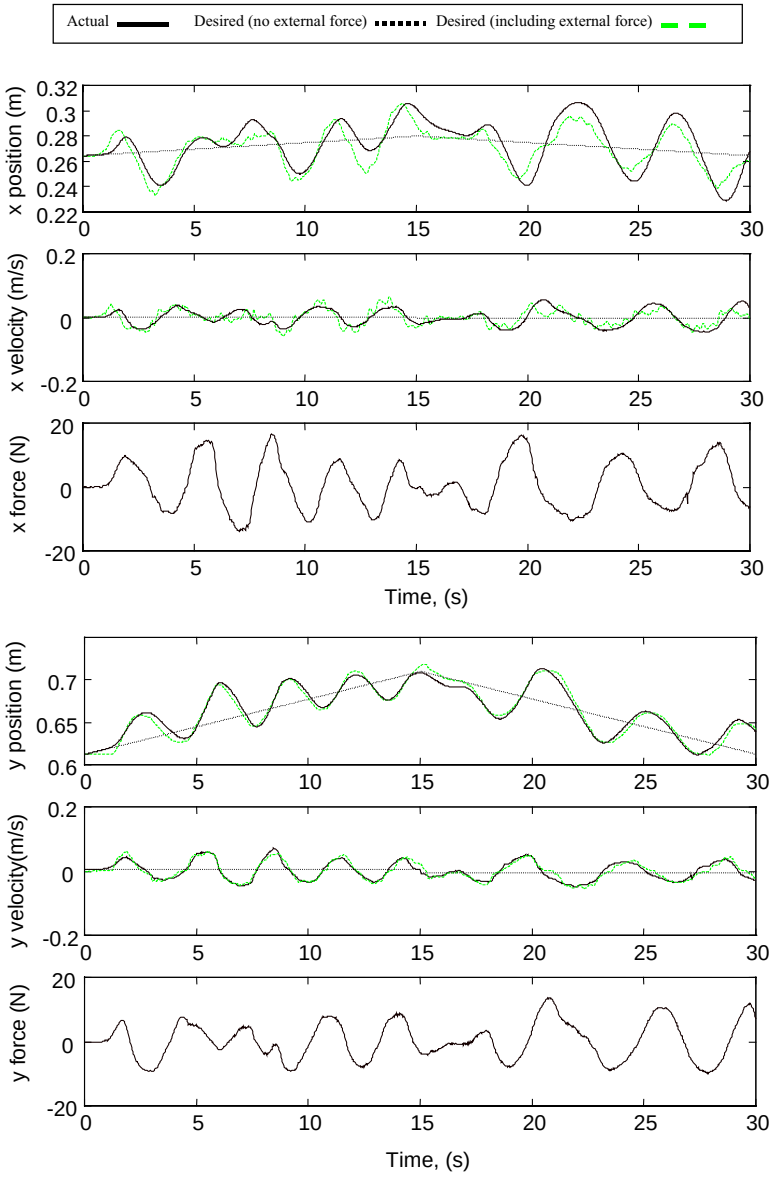

Fig. 14. Pole-placement impedance controller ($K = 250$, $C = 250$).

7. Conclusions

An impedance controller for a pneumatic robot is presented here based around joint-space pole-placement position controllers. The impedance control strategy has been successfully implemented on the robot.

Due to the robot configuration a linearising strategy has been implemented to improve the performance of the joint space controllers. The increased linearisation has enabled an optimisation strategy to improve the PID joint space response. Moreover the increased linearity has enabled pole-placement (a model-based linear controller) to be implemented on the individual joints, improving the step response by decreasing the rise time and reducing the overshoot. It may have been possible to implement a pole-placement controller on the original system without linearisation however this would severely effect the controller robustness to measurement errors. Control signal saturation also effected the performance of the joint space controllers, requiring the speed of the closed-loop poles to be restricted. Faster poles result in larger control signals, which would breach the saturation limit and result in poor controller performance or instability. Actuating link 2 with two pneumatic actuators, rather than one, would increase the force output enabling higher force outputs before controller saturation.

Combination of the two joint space controllers using inverse kinematics enabled x and y position tracking of the robot end-point. The robot tracked the desired position with a small error. The error is a result of the fore-mentioned control signal saturation problem.

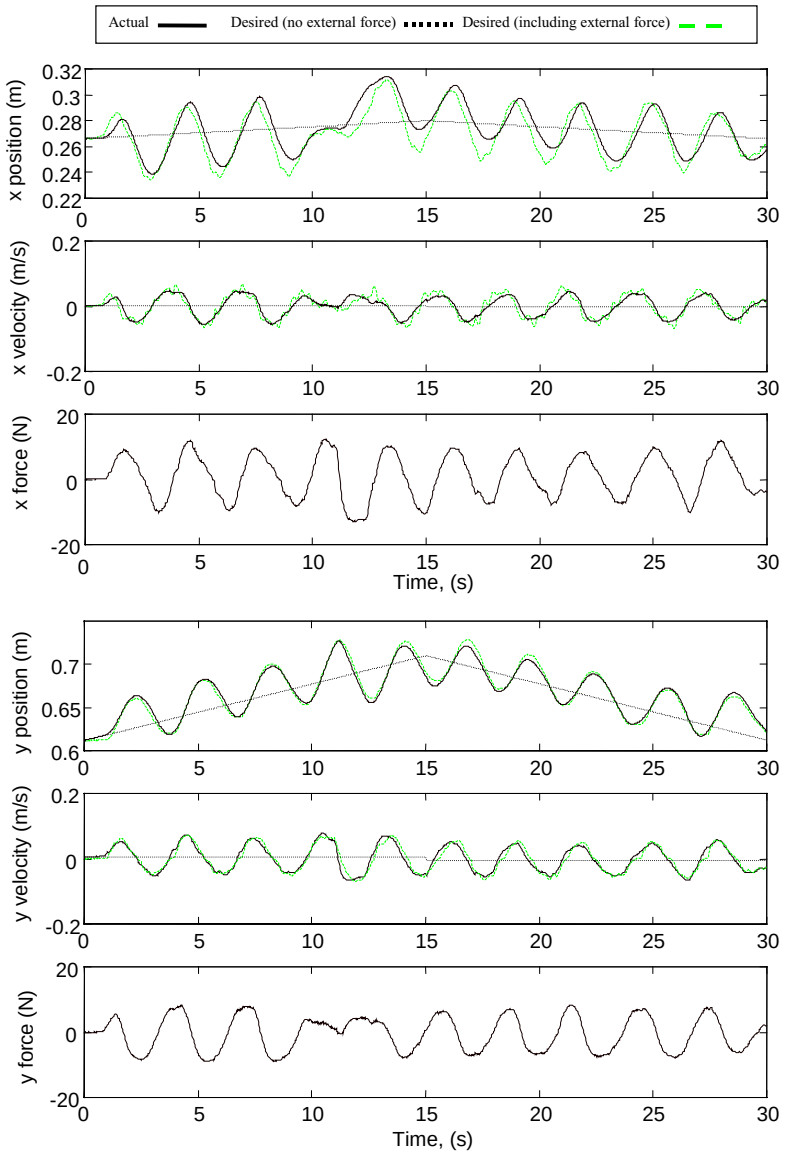

Fig. 15. Pole-placement impedance controller ($K = 130$, $C = 130$).

The impedance controller was implemented successfully and enabled the robot to respond differently to similar levels of input force. The large values of stiffness and damping produced the poorest response due to increased errors in force measurement and as larger forces are a more extreme measure of controller performance. Increasing the stiffness of the impedance characteristics results in the robot applying larger forces to achieve the desired trajectory. Increasing the damping restricts large velocities even if the robot is not in the correct position. In a physiotherapy context stiffness will be used to assist the patient toward the required position. Patients with low ability will perform the exercises with high stiffness. The stiffness will be decreased with the patients increasing ability. The damping will be set depending upon the level of tremors the patient experiences during motion. Both the stiffness and damping will be specified by a trained physiotherapist to ensure the correct therapy is implemented.

The force sensor is the crux of the entire control strategy with errors in measurement resulting in an incorrect impedance response being implemented but also providing an incorrect signal for the open-loop force controllers. The force sensor used in these experiments is custom made and susceptible to error in force measurement when torque is applied. Overall the control strategy performed well enabling safe robot/human interaction. Future work will improve the multiple degree of freedom force sensor, improve the response of the joint space controllers and test the robot on a few sample patients.

References

Astrom, K. J. & Wittenmark, B. (1997). *Computer-controlled systems, theory and design*. Englewood Cliffs, NJ: Prentice-Hall, ISBN 0-13-314899-8.

Chiavervini, S., & Sciavicco, L. (1993). The parallel approach to force/position control of robotic manipulators. *IEEE Transactions on Robotics and Automation*, *9*(4), 361–373.

Ferretti, G., Magnani, G., & Rocco, P. (1997). Towards the implementation of hybrid force/position control in industrial robots. *IEEE Transactions on Robotics and Automation*, *13*(6), 838–845.

Gorce, P., & Guihard, M. (1999). Joint impedance pneumatic control for multilink systems. *ASME Journal of Dynamic Systems, Measurement and Control*, *121*, 293–297.

Heinrichs, B., Sepehri, N., & Thorton-Trump, A. B. (1997). Position-based impedance control of an industrial hydraulic manipulator. *IEEE Control Systems Magazine (special issue on Robotics and Automation)*, *17*, 46–52.

Hogan, N. (1985). Impedance control: An approach to manipulation part I, II, III. *Journal of Dynamic Systems, Measurements and Control,*, *107*(1), 1–24.

Krebs, H. I., Hogan, N., Aisen, M. L., & Volpe, B. T. (1998). Robot-aided neuro-rehabilitation. *IEEE Transactions on Rehabilitation Engineering*, *6*(1), 75–87.

Ling, C., & Plummer, A. R. (1999). Stability and robustness for discrete-time systems, with control signal saturation. *Proceedings of the Institution of Mechanical Engineers*, *214*(Part 1), 65–76.

Liu, S., & Bobrow, J. E. (1988). An analysis of a pneumatic servo system and it's application to a computer-controlled robot. *Transactions of ASME Journal of Dynamic Systems Measurements and Control*, *110*, 228–235.

Noritsugu, T. & Yamanaka, T. (1996). Application of Rubber Artificial Muscle Manipulator as a Rehabilitation Robot. *Proceedings of the fifth IEEE international workshop on robot and human communication* (pp. 112–117), Japan.

Richardson, R. (2001). *Control and actuation for robotic physiotherapy*. Ph.D. Thesis. University of Leeds, UK.

Richardson, R., Brown, M. D., Bhakta, B., & Levesley, M. C. (2003). Design and control of a three degree of freedom pneumatic physiotherapy robot. *Robotica*, *21*, 589–604.

Richardson, R., Brown, M. D. & Plummer, A. R. 2000. Pneumatic impedance control for physiotherapy. *Proceedings of the European advanced robotics systems—Robotics 2000*, University of Salford, 12–14 April.

Richardson, R., Plummer, A. R., & Brown, M. D. (2001). Self-tuning control of a low friction pneumatic actuator under the influence of gravity. *IEEE Transactions on Control Systems Technology*, *9*(2), 330–334.

Schutter, J. D., & Brussel, H. (1987). Compliant robot motion II: A control strategy based upon external control loops. *The International Journal of Robotic Research*, *7*(4), 18–33.

Vaughan, N. D., & Plummer, A. R. (1990). Robust adaptive control for hydraulic servo-systems. *Proceedings of the ASME winter annual meeting* (pp. 2–9), November.